

## Supporting Information

# Facile Syntheses of Silver Thioantimonates Exhibiting Second-harmonic Generation Responses and Large Birefringence

Gang Yang,<sup>a,b,#</sup> Xingxing Jiang,<sup>c,#</sup> Chao Wu,<sup>b,#</sup> Zheshuai Lin,<sup>c</sup> Zhipeng Huang,<sup>b</sup>  
Mark G. Humphrey<sup>d</sup> and Chi Zhang\*,<sup>a,b</sup>

<sup>a</sup> China-Australia Joint Research Center for Functional Molecular Materials, School of Chemical and Material Engineering, Jiangnan University, Wuxi 214122, P. R. China

<sup>b</sup> School of Chemical Science and Engineering, Tongji University, Shanghai 200092, P. R. China

<sup>c</sup> Key Lab of Functional Crystals and Laser Technology, Technical Institute of Physics and Chemistry, Chinese Academy of Sciences, Beijing 100190, China

<sup>d</sup> Research School of Chemistry, Australian National University, Canberra, ACT 2601, Australia

**Table S1.** Atomic coordinates ( $\times 10^4$ ) and equivalent isotropic displacement parameters ( $\text{\AA}^2 \times 10^3$ ) for [enH<sub>2</sub>][Ag<sub>4</sub>Sb<sub>2</sub>S<sub>6</sub>] and [enH][Ag<sub>2</sub>SbS<sub>3</sub>].

**Table S2.** Selected bond distances ( $\text{\AA}$ ) and angles (deg) for [enH<sub>2</sub>][Ag<sub>4</sub>Sb<sub>2</sub>S<sub>6</sub>].

**Table S3.** Selected bond distances ( $\text{\AA}$ ) and angles (deg) for [enH][Ag<sub>2</sub>SbS<sub>3</sub>].

**Table S4.** Hydrogen-bonding interactions for [enH<sub>2</sub>][Ag<sub>4</sub>Sb<sub>2</sub>S<sub>6</sub>].

**Table S5.** Hydrogen-bonding interactions for [enH][Ag<sub>2</sub>SbS<sub>3</sub>].

**Table S6.** Calculated NLO properties for [enH][Ag<sub>2</sub>SbS<sub>3</sub>] deduced from real-space atom-cutting analysis.

**Figure S1.** Experimental (red) and simulated (blue) powder X-ray diffraction patterns for [enH<sub>2</sub>][Ag<sub>4</sub>Sb<sub>2</sub>S<sub>6</sub>] (a) and [enH][Ag<sub>2</sub>SbS<sub>3</sub>] (b).

**Figure S2.** Energy dispersive spectroscopy results of [enH<sub>2</sub>][Ag<sub>4</sub>Sb<sub>2</sub>S<sub>6</sub>] (a) and [enH][Ag<sub>2</sub>SbS<sub>3</sub>] (b).

**Figure S3.** Infrared spectra of [enH<sub>2</sub>][Ag<sub>4</sub>Sb<sub>2</sub>S<sub>6</sub>] (a) and [enH][Ag<sub>2</sub>SbS<sub>3</sub>] (b).

## References

**Theoretical Calculations:** The bandgap calculated by standard DFT is inconsistent with the experimental data due to the discontinuity in the exchange-correlation functional, so a scissor operator<sup>S1</sup> was used to shift the conduction band upward to agree with the measured value. Based on the scissor-operator-corrected electronic band structure, the imaginary part of the dielectric function from the electronic transition between the valence band (VB) and the conduction band (CB) can be calculated. The real part of the dielectric function, i.e., the refractive indices, can be determined by a Kramers-Kronig transform.<sup>S2</sup> The anisotropic SHG coefficients were calculated by the program developed by our group.<sup>S3,S4</sup> To investigate the contribution of the constituent groups to the SHG effect, real-space atom-cutting analysis was performed on the crystals.<sup>S5,S6</sup> In real-space atom-cutting analysis, when the contribution to the optical properties of a specified ion (or group) is of interest, the wavefunction in the zones belonging to the other ions (groups) is set to zero (which is referred to as “atom cutting”). The contribution of the ion (group) of interest to the  $n$ -th polarizability is  $\chi^n(X) = \chi^n$  (all the atoms are cut except  $X$ ). In the SHG-weighted electronic cloud calculations, the probability densities of all occupied (valence) or unoccupied (conduction) states projected onto the real space are multiplied by a weighting factor that is related to the contribution to the SHG efficiency by the virtual electron (VE) and virtual hole (VH) processes.<sup>S6</sup> This ensures that the quantum states irrelevant to SHG are not shown in the occupied or unoccupied “SHG-densities”, while the orbitals vital to SHG are intuitively highlighted in the real space.

**Table S1.** Atomic coordinates ( $\times 10^4$ ) and equivalent isotropic displacement parameters ( $\text{\AA}^2 \times 10^3$ ) for [enH<sub>2</sub>][Ag<sub>4</sub>Sb<sub>2</sub>S<sub>6</sub>] and [enH][Ag<sub>2</sub>SbS<sub>3</sub>]. U(eq) is defined as one third of the trace of the orthogonalized U<sub>ij</sub> tensor.

atom	x	y	z	U <sub>eq</sub> ( $\text{\AA}^2$ )
<b>[enH<sub>2</sub>][Ag<sub>4</sub>Sb<sub>2</sub>S<sub>6</sub>]</b>				
Sb(1)	3656(1)	1892(1)	528(1)	15(1)
Ag(1)	6216(1)	1795(1)	6707(1)	34(1)
Ag(2)	9527(1)	1867(1)	4474(1)	45(1)
S(1)	5948(3)	1093(1)	3448(3)	19(1)
S(2)	2950(3)	1171(1)	-2590(3)	21(1)
S(3)	-133(3)	1862(1)	559(3)	20(1)
N(1)	7230(20)	220(7)	10080(20)	27(3)
N(2)	9480(30)	-227(9)	7170(30)	47(4)
C(1)	8850(17)	58(5)	9011(18)	46(2)
<b>[enH][Ag<sub>2</sub>SbS<sub>3</sub>]</b>				
Sb(1)	-7799(1)	-1043(1)	-3050(1)	14(1)
Ag(1)	-11907(2)	-1040(1)	-8136(2)	32(1)
Ag(2)	-5938(2)	-1166(1)	-7194(2)	30(1)
S(1)	-8367(5)	-2320(2)	-5779(4)	18(1)
S(2)	-11922(5)	-1005(2)	-3479(5)	20(1)
S(3)	-5775(5)	-2291(2)	-100(4)	16(1)
N(1)	-2905(19)	-6177(8)	-184(17)	34(3)
N(2)	-1297(18)	-3432(7)	-979(15)	25(2)
C(1)	-3320(20)	-5133(9)	-1114(17)	24(3)
C(2)	-900(20)	-4461(10)	28(18)	28(3)

**Table S2.** Selected bond distances ( $\text{\AA}$ ) and angles (deg) for  $[\text{enH}_2][\text{Ag}_4\text{Sb}_2\text{S}_6]$ .

Sb(1)-S(2)	2.4059(18)	Sb(1)-S(1)	2.4167(18)
Sb(1)-S(3)	2.4444(18)	Ag(1)-S(1)	2.5427(18)
)			
Ag(1)-S(3)#2	2.5878(19)	Ag(1)-S(2)#3	2.653(2)
Ag(2)-S(1)	2.5628(19)	Ag(2)-S(3)#5	2.569(2)
Ag(2)-S(2)#2	2.569(2)	Ag(2)-S(3)#6	2.770(2)
N(1)-C(1)	1.554(17)	N(2)-C(1)	1.583(19)
C(1)-C(1)#11	1.485(19)		
S(2)-Sb(1)-S(1)	98.17(6)	S(2)-Sb(1)-S(3)	102.16(6)
S(1)-Sb(1)-S(3)	102.00(6)	S(1)-Ag(1)-S(3)#2	125.02(6)
S(1)-Ag(1)-S(2)#3	99.73(6)	S(3)#2-Ag(1)-S(2)#3	105.21(6)
S(1)-Ag(2)-S(3)#5	126.43(6)	S(1)-Ag(2)-S(2)#2	103.75(6)
S(3)#5-Ag(2)-S(2)#2	111.00(6)	S(1)-Ag(2)-S(3)#6	101.28(6)
S(3)#5-Ag(2)-S(3)#6	104.21(5)	S(2)#2-Ag(2)-S(3)#6	109.00(6)
Sb(1)-S(1)-Ag(1)	97.95(6)	Sb(1)-S(1)-Ag(2)	88.41(6)
Ag(1)-S(1)-Ag(2)	75.77(5)	Sb(1)-S(2)-Ag(2)#7	96.95(7)
Sb(1)-S(2)-Ag(1)#8	92.74(6)	Ag(2)#7-S(2)-Ag(1)#8	94.67(6)
Sb(1)-S(3)-Ag(2)#9	85.81(6)	Sb(1)-S(3)-Ag(1)#7	115.60(7)
Ag(2)#9-S(3)-Ag(1)#7	80.84(6)	Sb(1)-S(3)-Ag(2)#10	121.97(7)
Ag(2)#9-S(3)-Ag(2)#10	103.80(7)	Ag(1)#7-S(3)-Ag(2)#10	122.41(7)

Symmetry transformations used to generate equivalent atoms: #1  $x, -y+1/2, z-1/2$ , #2  $x+1, y, z+1$ , #3  $x, y, z+1$ , #4  $x, -y+1/2, z+1/2$ , #5  $x+1, -y+1/2, z+1/2$ , #6  $x+1, y, z$ , #7  $x-1, y, z-1$ , #8  $x, y, z-1$ , #9  $x-1, -y+1/2, z-1/2$ , #10  $x-1, y, z$ , #11  $-x+2, -y, -z+2$ .

**Table S3.** Selected bond distances ( $\text{\AA}$ ) and angles (deg) for [enH][Ag<sub>2</sub>SbS<sub>3</sub>].

Sb(1)-S(2)	2.412(3)	Sb(1)-S(1)	2.420(3)
Sb(1)-S(3)	2.430(3)	Ag(1)-S(2)#2	2.457(3)
Ag(1)-S(1)	2.536(3)	Ag(1)-S(3)#3	2.581(3)
Ag(2)-S(3)#5	2.583(3)	Ag(2)-S(1)	2.611(3)
Ag(2)-S(2)#6	2.660(3)	N(1)-C(1)	1.388(13)
C(1)-C(2)	1.533(15)	N(2)-C(2)	1.397(13)
S(2)-Sb(1)-S(1)	101.11(10)	S(2)-Sb(1)-S(3)	100.00(10)
S(1)-Sb(1)-S(3)	99.51(10)	S(2)#2-Ag(1)-S(1)	129.03(10)
S(2)#2-Ag(1)-S(3)#3	124.25(10)	S(1)-Ag(1)-S(3)#3	106.66(10)
Sb(1)-S(1)-Ag(1)	85.25(10)	Sb(1)-S(1)-Ag(2)	97.36(10)
Ag(1)-S(1)-Ag(2)	82.93(9)	Sb(1)-S(2)-Ag(1)#1	93.16(10)
Sb(1)-S(2)-Ag(2)#4	121.61(12)	Ag(1)#1-S(2)-Ag(2)#4	97.68(10)
Sb(1)-S(3)-Ag(1)#7	94.41(10)	Sb(1)-S(3)-Ag(2)#8	102.59(10)
Ag(1)#7-S(3)-Ag(2)#8	68.48(8)		

Symmetry transformations used to generate equivalent atoms: #1 x, -y, z+1/2, #2 x, -y, z-1/2, #3 x-1, y, z-1, #4 x-1, y, z, #5 x, y, z-1, #6 x+1, y, z, #7 x+1, y, z+1, #8 x, y, z+1.

**Table S4.** Hydrogen-bonding interactions for [enH<sub>2</sub>][Ag<sub>4</sub>Sb<sub>2</sub>S<sub>6</sub>].

D—H···A	<i>d</i> (D—H)	<i>d</i> (H···A)	<i>d</i> (D···A)	$\angle$ (DHA)
N1—H1A···S1	0.9600	2.6700	3.2501	119.00
N1—H1B···S2	0.9600	2.1600	3.1129	170.00
N1—H1E···S2	0.9600	2.3800	3.2385	148.00
N2—H2A···S2	0.9600	2.8500	3.4817	124.00
N2—H2B···S2	0.9600	2.8100	3.3220	114.00
N2—H2C···S1	0.9600	2.7200	3.5897	151.00
C1—H1C···S1	0.9600	2.8600	3.5478	136.00

**Table S5.** Hydrogen-bonding interactions for [enH][Ag<sub>2</sub>SbS<sub>3</sub>].

D—H···A	<i>d</i> (D—H)	<i>d</i> (H···A)	<i>d</i> (D···A)	$\angle$ (DHA)
N1—H1A···S1	0.8600	2.6900	3.5399	171.00
N1—H1B···S1	0.8900	2.8100	3.6580	160.00
N2—H2B···S3	0.8900	2.5800	3.4308	161.00
N2—H2C···S3	0.8900	2.5500	3.4272	167.00

**Table S6.** Calculated NLO properties for [enH][Ag<sub>2</sub>SbS<sub>3</sub>] deduced from real-space atom-cutting analysis.<sup>a</sup>

	d <sub>11</sub>	d <sub>12</sub>	d <sub>13</sub>	d <sub>15</sub>	d <sub>24</sub>	d <sub>33</sub>
all	-25.21	-4.64	5.27	12.17	1.68	-9.58
[Ag(1)S <sub>3</sub> ]	-15.68	-2.62	3.65	6.58	0.12	-3.36
[Ag(2)S <sub>3</sub> ]	-17.88	-1.65	2.68	8.32	0.98	-6.77
[SbS <sub>3</sub> ]	-20.35	-2.88	2.11	9.68	1.39	-6.68
[NH <sub>2</sub> CH <sub>2</sub> CH <sub>2</sub> NH <sub>3</sub> ] <sup>+</sup>	0.21	-0.08	0.06	0.16	0.05	0.09

<sup>a</sup>d values in pm/V

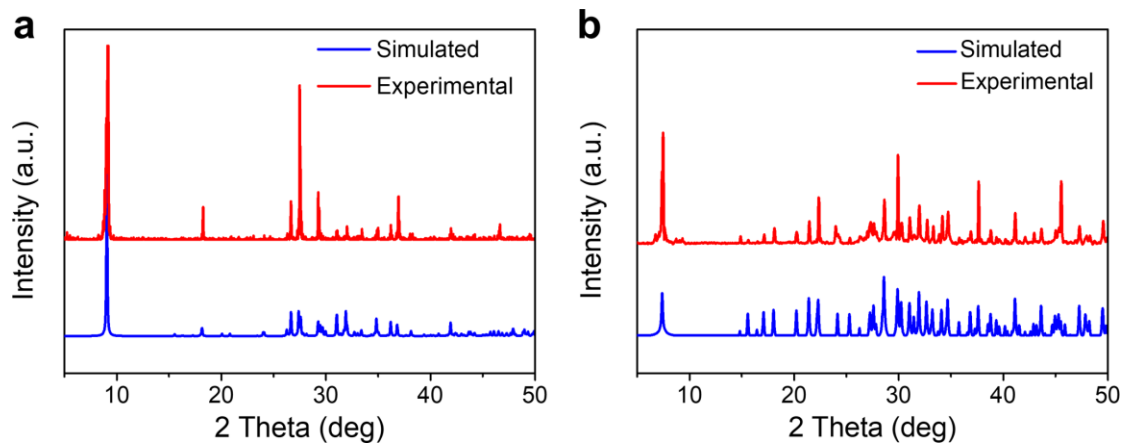


**Figure S1.** Experimental (red) and simulated (blue) powder X-ray diffraction patterns for  $[enH_2][Ag_4Sb_2S_6]$  (a) and  $[enH][Ag_2SbS_3]$  (b).

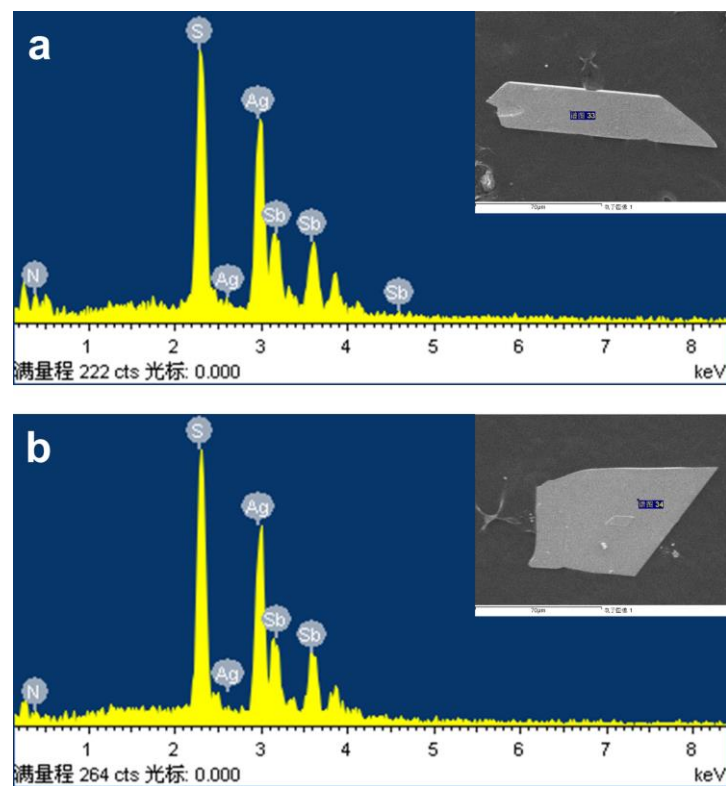


**Figure S2.** Energy dispersive spectroscopy results of  $[enH_2][Ag_4Sb_2S_6]$  (a) and  $[enH][Ag_2SbS_3]$  (b).

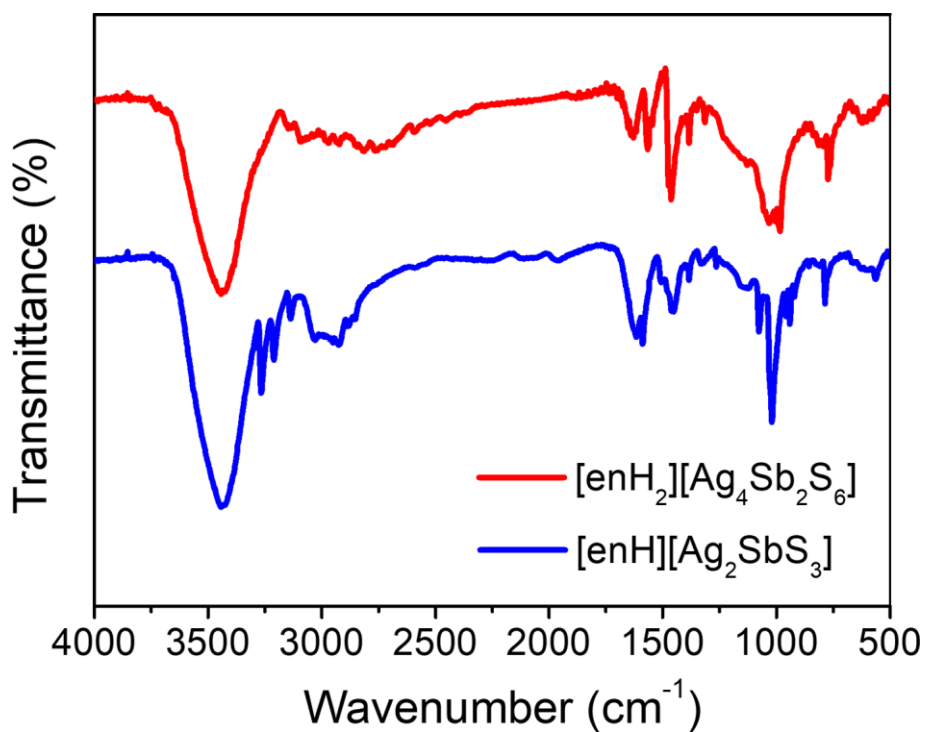


**Figure S3.** Infrared spectra of  $[\text{enH}_2]\text{[Ag}_4\text{Sb}_2\text{S}_6]$  (a) and  $[\text{enH}]\text{[Ag}_2\text{SbS}_3]$  (b).

## References

- (S1) R. W. Godby, M. Schlüter and L. J. Sham, *Phys. Rev. B: Condens. Matter Mater. Phys.*, 1988, **37**, 10159–10175.
- (S2) E. D. Palik, *Handbook of Optical Constants of Solids*; Academic: New York, 1985.
- (S3) Z. S. Lin, X. X. Jiang, L. Kang, P. F. Gong, S. Luo and M. H. Lee, *J. Phys. D: Appl. Phys.*, 2014, **47**, 253001.
- (S4) J. Lin, M. H. Lee, Z. P. Liu, C. Chen and C. J. Pickard, *Phys. Rev. B: Condens. Matter Mater. Phys.*, 1999, **60**, 13380–13389.
- (S5) R. He, Z. S. Lin, M. H. Lee and C. T. Chen, *J. Appl. Phys.*, 2011, **109**, 103510.
- (S6) M. H. Lee, C. H. Yang and J. H. Jan, *Phys. Rev. B: Condens. Matter Mater. Phys.*, 2004, **70**, 235110.